Biol. Cybern. 76, 107–117 (1997)

Biological Cybernetics

Analysis of an optimal control model of multi-joint arm movements

Ning Lan

Biomedical Engineering and Instrumentation, Department of Electrical Engineering, Tsinghua University, Beijing 100084, People's Republic of China

Received: 4 December 1995 / Accepted in revised form: 17 September 1996

Abstract. In this paper, we propose a model of biological motor control for generation of goal-directed multi-joint arm movements, and study the formation of muscle control inputs and invariant kinematic features of movements. The model has a hierarchical structure that can determine the control inputs for a set of redundant muscles without any inverse computation. Calculation of motor commands is divided into two stages, each of which performs a transformation of motor commands from one coordinate system to another. At the first level, a central controller in the brain accepts instructions from higher centers, which represent the motor goal in the Cartesian space. The controller computes joint equilibrium trajectories and excitation signals according to a minimum effort criterion. At the second level, a neural network in the spinal cord translates the excitation signals and equilibrium trajectories into control commands to three pairs of antagonist muscles which are redundant for a two-joint arm. No inverse computation is required in the determination of individual muscle commands. The minimum effort controller can produce arm movements whose dynamic and kinematic features are similar to those of voluntary arm movements. For fast movements, the hand approaches a target position along a near-straight path with a smooth bell-shaped velocity. The equilibrium trajectories in X and Y show an 'N' shape, but the end-point equilibrium path zigzags around the hand path. Joint movements are not always smooth. Joint reversal is found in movements in some directions. The excitation signals have a triphasic (or biphasic) pulse pattern, which leads to stereotyped triphasic (or biphasic) bursts in muscle control inputs, and a dynamically modulated joint stiffness. There is a fixed sequence of muscle activation from proximal muscles to distal muscles. The order is preserved in all movements. For slow movements, it is shown that a constant joint stiffness is necessary to produce a smooth movement with a bell-shaped velocity. Scaled movements can be reproduced by varying the constraints on the maximal level of excitation signals according to the speed of movement. When the inertial parameters of the arm are altered, movement trajectories can be kept invariant by adjusting the pulse height values, showing the ability to adapt to load changes. These results agree with a wide range of experimental observations on human voluntary movements.

1 Introduction

In multi-joint arm movements performed by humans, the coordination strategy for a set of redundant muscles and the consequent invariant features of movements are not well understood. Hierarchical structure of the biological motor system is appealing because it provides a framework of sequential computation for motor commands. Unfortunately, the computational sequence from movement trajectory to joint torques and then to muscle control inputs yields no unique solution for the excessive degrees of freedom and the redundant muscles in a biological motor system (Hildreth and Hollerbach 1987; Hasan 1991). Since the movement trajectory is relatively insensitive to changes in muscle activation pattern, uncertainty may also be introduced in the determination of a particular muscle activation sequence from the given movement trajectory. An alternative which avoids the computational difficulty seems to lie in the use of a muscle-inherent biomechanical property. It has been suggested that the brain may utilize the spring-like nature of muscle to simplify computation of motor commands. A movement may be initiated by setting appropriate stiffness field of the limb, while shifting the equilibrium point of the joint, which is known as the equilibrium point (EP) control hypothesis (Feldman 1986; Bizzi et al. 1992). However, it is unclear how the activation of each muscle is assigned so that an appropriate stiffness field is produced, and how the equilibrium point is shifted in time in order to lead the joint to the final destination. There is also a lack of understanding with regard to the conversion of central commands to peripheral muscle inputs. Thus, the EP hypothesis remains dissociated from the large volume of existing

Correspondence: e-mail: thudjln@sp.net.edu.cn

experimental data concerning voluntary arm movements. This study is an attempt to bridge the gap from EP control theory to experimental observations.

Extensive experimental studies have been carried out to identify biological control strategies of movements. One class of models based on experimental observations focuses on the triphasic muscle activation pattern which is evident for both single-joint and multi-joint movements (Lestienne 1979; Ghez and Martin 1982; Marsden et al. 1983; Hannaford and Stark 1985; Karst and Hasan, 1991a,b; Flanders et al. 1994). In the impulse-timing model, Wallace (1981) assumed that a motor program could calculate the timing and duration of excitation pulses for the agonist and antagonist muscles. In the dual strategy model, a motor program was postulated to modulate the heights and durations of the excitation pulses, so that a class of scaled arm movements could be produced (Gottlieb et al. 1989; Corcos et al. 1989). An optimal algorithm was also used to search for the best timing and amplitude parameters of the triphasic activation pulses (Hannaford and Stark 1987). An elaborated biomechanical model of a pair of antagonistic muscles was developed to investigate the control of single-joint movements by a multiple objective function (Seif-Naraghi and Winters 1990). These models illustrated the essential role of a triphasic activation pattern in controlling single joint movements.

Optimal criteria for the formation of movement trajectories are also proposed to account for the invariant kinematics of arm movements. Voluntary arm movements appear invariant, with a characteristic near-straight hand path and a bell-shaped velocity profile in Cartesian space (Morasso 1981; Abend et al. 1982; Flash and Hogan 1985; Hogan 1988; Atkeson and Hollerbach, 1985). It is suggested that a plausible objective for planning the trajectory is that the movement produced should be as smooth as possible. This objective can best be described as minimizing the jerk of movements (Flash and Hogan 1985). The minimal jerk trajectory has an invariant kinematics that does not change under the perturbation of an external load, since the optimal trajectory is not dependent explicitly on limb dynamics. It was observed that the kinematics of human arm movement was not altered when the hand was subjected to an external force perturbation (Shadmehr and Mussa-Ivaldi 1994). An alternative to minimizing jerk in the planning of movement is to minimize the total torque changes during movements (Uno et al. 1989; Kawato et al. 1990). This criterion is able to prescribe an optimal trajectory with a slightly curved hand path, but cannot explain the trajectory invariance observed under the perturbation of external forces, since the minimal torque change trajectory explicitly depends on limb dynamics. Furthermore, an inverse computation is likely to be required to obtain control signals at the muscular level (Katayama and Kawato 1993).

A more robust objective function proposed for movement control is the minimal effort criterion (Hasan 1986). This objective function takes into account both movement kinematics and neuromuscular dynamics during movement. It is demonstrated that for an inertially-loaded single joint, an N-shaped equilibrium trajectory with an appropriate constant joint stiffness can produce a smooth movement with a bell-shaped velocity (Hasan, 1986). An elaborated model is developed that includes the spring-like property of muscle and spinal reciprocal control for antagonists (Lan and Crago 1994). With this model, the minimal effort criterion is able to reproduce all major features of single-joint movements, including an N-shaped equilibrium trajectory, a sigmoidal movement trajectory, the bell-shaped movement velocity, the triphasic burst pattern of agonist/antagonist muscle activation and a dynamically modulated joint stiffness. It is further demonstrated that a class of movement with a similar kinematic profile can also be obtained. These results agree with a large set of experimental data on single-joint movements.

Earlier studies (Hasan 1986; Lan and Crago 1994) have shown that the minimal effort criterion provides a teleological explanation for all regularities observed in single-joint movements. In the present paper, we extend the hierarchical model and the minimal effort criterion function to multi-joint movement control on the basis of the EP hypothesis. In the extended model, a spinal reciprocal neural circuit plays an essential part in the computation for agonist/antagonist muscle activations. We will address the following issues in the present study: (1) whether the minimal effort criterion is applicable to multi-joint arm movements, which is a much more general problem of biological movement control; (2) the formation of an invariant muscle activation pattern and movement kinematics in multi-joint movements; and (3) how these invariant characteristics are preserved under various conditions. We will first establish a neural control model for computing motor commands, which includes spinal reciprocal control for mono-articular as well as biarticular muscles. The minimal effort criterion is extended to describe multi-joint movements. A biomechanical model of a two-joint arm with three pairs of antagonistic muscles is used for simulation. The control problem is finally formulated as a dynamic optimization problem, which is solved by a numerical method. Numerical solutions of the optimization problem are analyzed. The results offer new insight into the planning and control of multi-joint arm movement by the brain.

2 Computation of motor commands

2.1 Objective function

The computation of motor commands follows a hierarchical structure illustrated in Fig. 1. It consists of a controller situated in the brain, a neural network in the spinal cord and a two-joint arm that is shown in Fig. 2. The goal of a movement is defined as transporting the hand from the initial position P_o to the target position, P_f, in Cartesian space. The motor goal is passed from the higher center in the brain to the controller as its inputs. A different input to the controller, Ph_i ($i = 1, 2, 3$), determines kinematic aspects of movements, such as the velocity profile and the overall speed of a movement.

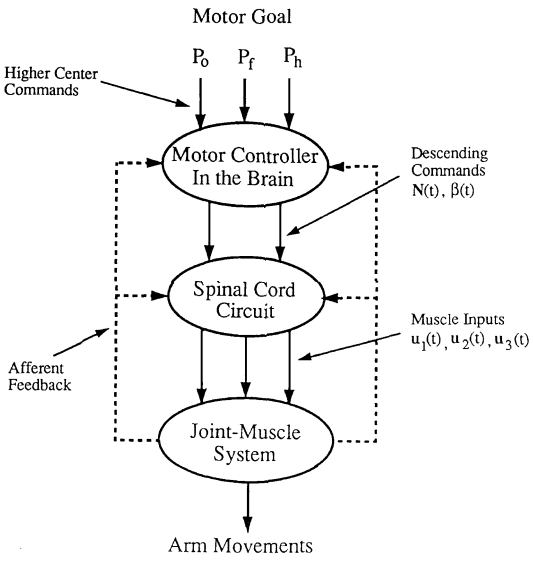

Fig. 1. The hierarchical structure of the model for movement control. The computation of motor commands is completed in two separate stages. The motor program located in the brain accepts inputs from higher centers of the brain and computes descending commands, which are then translated into muscle control inputs by a spinal cord circuit. Muscle inputs drive the arm to initiate a movement

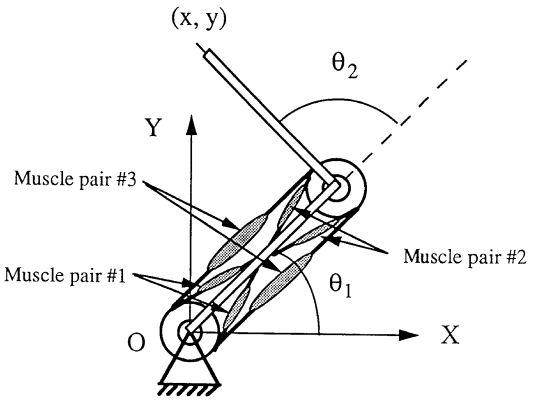

Fig. 2. The two-joint arm model. Three pairs of antagonist muscles are included: *pair #1* is shoulder muscles, *pair #2* is elbow muscles, *pair #3* is biarticular muslces. The moment arms of these muscles are assumed to be constant. The elbow and shoulder are assumed to be hinge joints

To address the suitability of the minimal effort criterion for control of multi-joint arm movements, we extend this objective function to a general form as follows:

$$J = \int_0^{t_f} \dot{\beta}(t)^T \mathbf{R}(t) \dot{\beta}(t)\, \mathrm{d}t \tag{1}$$

Here $\dot{\beta}(t)$ is the vector of equilibrium velocities, i.e., the time derivative of the equilibrium vector in the joint space, $\beta(t) = [\beta_1, \beta_2]^T$; $\mathbf{R}(t)$ is the joint stiffness matrix, which is a (2×2) symmetric, positive definite matrix in our case, and t_f is the duration of integration. The controller minimizes this objective function in the computation of its outputs, i.e., the excitation signal $N_i(t)$ $(i = 1, 2, 3)$ and the equilibrium points $\beta_1(t)$ and $\beta_2(t)$.

2.2 Spinal computation of muscle control inputs

The spinal neural circuit involved in computing muscle inputs from the descending signals is a reciprocal inhibition network mediated by Ia afferents. We assume that the stretch reflex plays a role in maintaining muscle's invariant spring-like property (Feldman and Orlovsky, 1972; Feldman, 1986).

At the spinal cord, the excitation signal, $N_i(t)$, causes a level of background activation in the motoneuron pools of a pair of antagonistic muscles. This process can be described by a first-order equation:

$$\frac{\mathrm{d}c_i(t)}{\mathrm{d}t} = -\frac{1}{\tau_{N_i}} c_i(t) + \frac{1}{\tau_{N_i}} N_i(t)$$
$$(0 \leqslant N_i(t) \leqslant 1, \text{ for } i = 1, 2, 3) \tag{2}$$

where i indicates the muscle pair number, $c_i(t)$ represents the background activation of the motoneuron pool of the i^{th} pair of muscles, $N_i(t)$ denotes the excitation signal to the i^{th} pair of muscles, and τ_{N_i} is the time constant of excitation.

The control inputs for single-joint muscles are determined as follows (Lan and Crago, 1994):

$$u_{i\mathrm{f}}(t) = c_i(t)\,[0.5 + r_{i\mathrm{f}}(\beta_i(t) - \theta_i(t))] \tag{3}$$

$$u_{i\mathrm{e}}(t) = c_i(t)\,[0.5 - r_{i\mathrm{e}}(\beta_i(t) - \theta_i(t))] \quad (\text{for } i = 1, 2) \tag{4}$$

For biarticular muscles, their inputs are determined differently as:

$$u_{3\mathrm{f}}(t) = c_3(t)\,[0.5 + r_{3\mathrm{f}}((\beta_1(t) - \theta_1(t)) + (\beta_2(t) - \theta_2(t)))] \tag{5}$$

$$u_{3\mathrm{e}}(t) = c_3(t)\,[0.5 - r_{3\mathrm{e}}((\beta_1(t) - \theta_1(t)) + (\beta_2(t) - \theta_2(t)))]$$
$$(0 \leqslant c_i(t) \leqslant 1; \text{ for } i = 1, 2, 3) \tag{6}$$

where subscript 'e' represents extensor muscle, and 'f' represents flexor muscle (see Sect. 3 for definition of flexor and extensor muscles), $u_{i\mathrm{f}}(t)$ and $u_{i\mathrm{e}}(t)$ are the control inputs to the flexor and extensor muscles, and r_{ij} $(j = \mathrm{f}, \mathrm{e})$ is the gain of reciprocal inhibition. The value of muscle inputs is thus confined between 0 and 1 (or $0 \leqslant u_{ij}(t) \leqslant 1$).

Equations (1)–(6) define the computation performed by the controller and the spinal reciprocal inhibition network. It is noted that in these processes no inverse computation is required. The information that is needed to determine muscle control inputs accurately is the motor goal and the afferent feedback. If afferent feedback is disabled, the ability to generate muscle control commands is not completely destroyed. By adjusting the descending commands, it may still be possible to perform some simple movements.

3 Biomechanical model of the arm

The biomechanical model of the two-joint arm is shown in Fig. 2. It consists of two rigid segments, and two hinge joints representing the shoulder and elbow. Movements are produced by three pairs of antagonistic muscles. Two pairs are single-joint muscles, crossing the shoulder joint (pair #1) and the elbow joint (pair #2). The third pair (#3) consists of biarticular muscles which cross both the shoulder and the elbow joints. In this study, we define a single-joint muscle that causes a counterclockwise rotation of the joint as a flexor, and a muscle that causes a clockwise joint rotation as an extensor. A biarticular muscle that tends to give rise to counterclockwise rotations of both joints described as a biarticular flexor; and a biarticular muscle that tends to elicit clockwise rotations of both joints as a biarticular extensor. All these definitions are given under isometric conditions.

The spring-like property of a muscle is approximated by a linear relation between its stiffness and the torque that it generates (Cannon and Zahalak 1982; Kearny and Hunter1990; Carter et al. 1993):

$$t_{ij}(t) = m_{ij}k_{ij} + b_{ij}; \quad (\text{for } i = 1, 2, 3 \text{ and } j = \text{f, e}) \tag{7}$$

Here t_{ij} is the torque produced by each muscle, k_{ij} is muscle stiffness, m_{ij} is a constant that determines the shape of torque-angle curve (Lan and Crago 1994), and b_{ij} is passive torque. The muscle stiffness is proportional to its activation, such that:

$$k_{ij}(t) = n_{ij}a_{ij}(t); \quad (0 \leqslant a_{ij} \leqslant 1) \tag{8}$$

where a_{ij} is muscle activation, and n_{ij} is the maximal muscle stiffness achieved at $a_{ij} = 1$.

Muscle activation dynamics is described by a first-order equation:

$$\frac{\mathrm{d}a_{ij}(t)}{\mathrm{d}t} = -\frac{1}{\tau_{ij}}a_{ij}(t) + \frac{1}{\tau_{ij}}u_{ij}(t); \quad (0 \leqslant a_{ij}(t) \leqslant 1, \text{ for } i = 1, 2, 3 \text{ and } j = \text{f, e}) \tag{9}$$

Here $u_{ij}(t)$ is neural control input to muscles given by eqs. (3)–(16) and τ_{ij} is the time constant of muscle activation.

Let us define K_i and t_i as the net joint stiffness and joint torque produced by each pair of muscles. Thus for the shoulder muscles (pair #1)

$$K_1(t) = k_{1\mathrm{f}}(t) + k_{1\mathrm{e}}(t); \quad t_1(t) = t_{1\mathrm{f}}(t) - t_{1\mathrm{e}}(t) \tag{10}$$

for the elbow muscles (pair #2)

$$K_2(t) = k_{2\mathrm{f}}(t) + k_{2\mathrm{e}}(t); \quad t_2(t) = t_{2\mathrm{f}}(t) - t_{2\mathrm{e}}(t) \tag{11}$$

and for the biarticular muscles (pair #3)

$$K_3(t) = k_{3\mathrm{f}}(t) + k_{3\mathrm{e}}(t); \quad t_3(t) = t_{3\mathrm{f}}(t) - t_{3\mathrm{e}}(t) \tag{12}$$

We assume here that biarticular muscles have equal moment arms at both joints. Thus, the joint stiffness matrix can be formed as:

$$\mathbf{R}(t) = \begin{bmatrix} K_1(t) + K_3(t) & K_3(t) \\ K_3(t) & K_2(t) + K_3(t) \end{bmatrix} \tag{13}$$

The cross elements in the joint stiffness matrix are due to biarticular muscles. The muscle torque vector is given by:

$$\begin{bmatrix} t_{1\mathrm{m}}(t) \\ t_{2\mathrm{m}}(t) \end{bmatrix} = \begin{bmatrix} t_1(t) + t_3(t) \\ t_2(t) + t_3(t) \end{bmatrix} \tag{14}$$

where $t_{1\mathrm{m}}(t)$ is the total muscle torque at the shoulder joint and $t_{2\mathrm{m}}(t)$ is the total muscle torque at the elbow joint.

The model takes into account the viscous property of muscle by a lumped viscous torque, which is proportional to joint stiffness (Cannon and Zahalak 1982; Flash 1987):

$$\begin{bmatrix} t_{1\mathrm{v}}(t) \\ t_{2\mathrm{v}}(t) \end{bmatrix} = -\delta[\mathbf{R}(t)] \begin{bmatrix} \dot{\theta}_1(t) \\ \dot{\theta}_2(t) \end{bmatrix} \tag{15}$$

where δ is a damping coefficient, $t_{1\mathrm{v}}$ and $t_{2\mathrm{v}}$ are the viscous torques at the shoulder and the elbow joints, and $\dot{\theta}_1(t)$ and $\dot{\theta}_2(t)$ are the angular velocities of the shoulder and elbow joints, respectively.

The total torque acting at each joint is thus the sum of active muscle torque and viscous torque:

$$\mathbf{T}(t) = \begin{bmatrix} T_1(t) \\ T_2(t) \end{bmatrix} = \begin{bmatrix} t_{1\mathrm{m}}(t) \\ t_{2\mathrm{m}}(t) \end{bmatrix} + \begin{bmatrix} t_{1\mathrm{v}}(t) \\ t_{2\mathrm{v}}(t) \end{bmatrix} \tag{16}$$

The dynamical equation of the arm is given by the following form (Paul 1981):

$$\mathbf{T}(t) = \mathbf{I}(\theta)\ddot{\theta} + \mathbf{C}(\theta, \dot{\theta})\dot{\theta} + \mathbf{g}(\theta) \tag{17}$$

Here $\mathbf{I}(\cdot)$ is the inertial matrix, which is symmetric, positive definite, and dependent on joint configuration; $\theta = [\theta_1, \theta_2]^T$ is the vector of joint angles; $\mathbf{C}(\cdot, \cdot)$ is the coupling matrix due to coriolis and centripetal forces; and $\mathbf{g}(\cdot)$ is the term due to the gravitational effects, which is neglected in planar movements.

4 Numerical method of optimization

4.1 Numerical technique

A numerical algorithm is employed to analyze the optimal behavior of multi-joint arm movement control. A software package, GAMS/MINOS, is used to obtain the numerical solution of the optimization problem. Details of this method are described in an earlier study of the single-joint model (Lan and Crago 1994).

In the multi-joint model the dimension of the system was greatly increased, and the nonlinearity of the system equations was much greater than that of the single-joint model. In order to improve numerical solvability, we chose state variables of the model carefully, and introduced intermediate variables to augment the state model. Numerical solution of the optimization problem was obtained on a CRAY C-90 supercomputer at the Pittsburgh Supercomputing Center. The values for muscle parameters and activation time constants were the same as used in Lan and Crago (1994). Limb parameters were similar to those used by Flash (1987). All parameter values used in numerical solutions are summarized in the Appendix.

4.2 Constraints

To obtain sensible numerical solutions, constraints on variables are imposed based on biomechanical and physiological considerations, so that the algorithm can converge to a solution more quickly and smoothly. The first constraint is the range of joint motion, which is limited to a feasible region, i.e.,

$$0^\circ \leqslant \theta_1, \theta_2 \leqslant 180^\circ \tag{18}$$

To satisfy constraints on muscle inputs and muscle stiffnesses in the numerical solution, it is more convenient to place constraints on the difference between the equilibrium trajectory and the actual trajectory. For single-joint muscles, the constraint takes the form

$$-\frac{1}{2r_{if}} \leqslant (\beta_i(t) - \theta_i(t)) \leqslant \frac{1}{2r_{ie}} \quad \text{for } i = 1, 2 \tag{19}$$

and for biarticular muscles, it is

$$-\frac{1}{2r_{3f}} \leqslant (\beta_1(t) - \theta_1(t)) + (\beta_2(t) - \theta_2(t)) \leqslant \frac{1}{2r_{3e}} \tag{20}$$

The constraints on the excitation signal, $N_i(t)$, are such that

$$0 \leqslant N_i(t) \leqslant Ph_i; \quad 0 < Ph_i \leqslant 1 \quad i = 1, 2, 3 \tag{21}$$

where Ph_i represents the maximum level of excitation signals, or the pulse heights. In the model, Ph_i is an independent input to the motor program from the higher center of the brain. Physiologically, it limits the maximal level of motoneuron pool excitation.

5 Results

5.1 Characteristics of a reaching movement

A reaching movement of 0.4 (s) duration from the left to the right direction at an angle of about 45° is investigated. The optimal hand movement in the X and Y directions and the corresponding equilibrium trajectories are presented in Fig. 3A. The hand movement in the Cartesian coordinates follows a near-straight path. Due to the dynamical effects in multi-joint limb, a perfectly straight hand movement is not possible. The equilibrium path is curved, and zigzags around the hand path with an overshoot to the final position. The velocity profiles are all bell-shaped, indicating a smooth movement in Cartesian space. In other simulations in which the hand path is severely curved, the bell-shaped velocity profile disappears, and sometimes double-peaked velocity occurs. The equilibrium trajectories in the X and Y directions clearly show the N-shaped pattern, similar to that in single joint movements (Hasan 1986; Lan and Crago 1994).

The characteristics of optimal joint movements are shown in Fig. 3B. The elbow movement is similar to that of single joint, having a smooth trajectory, a bell-shaped velocity and an N-shaped equilibrium trajectory. However, the shoulder movement is not all smooth. At the end of movement, there is a 'bump' in the velocity, indicating a reversal in the movement direction. Joint stiffness shows a double-peaked increase, one for acceleration and one for deceleration of the movement.

Optimal activation patterns for all three pairs of antagonists show triphasic characteristics, Fig. 3. This pattern corresponds to the three-pulsed optimal excitation of motoneuron pools. A certain degree of coactivation of antagonists is present, and co-contraction is more evident in the deceleration phase of the movement. The excitation pulses clearly illustrate differences in amplitude and timing of activation for the shoulder, elbow and biarticular muscles. The shoulder muscles are activated first, followed by the elbow muscles and biarticular muscles. This proximal to distal order of muscle activation is preserved for reaching movements in all directions.

5.2 Effects of excitation pulse height on movement kinematics

An appropriate level of excitation is necessary to produce the smoothest movement. This is illustrated in Fig. 4. To show this effect, we choose to vary the pulse height of elbow muscles from 0.05 to 0.6, while fixing the pulse heights of the shoulder and biarticular muscles at 0.3 and 0.2.

Figure 4 shows the hand paths and their velocity profiles, as well as the elbow pulse heights. It is clear among these movements, that the movement with a pulse height of 0.1 (illustrated by continuous line) has the straightest hand trajectory and the smoothest bell-shaped velocity. The pulse heights higher than 0.1 or lower than 0.1 give rise to more curved hand trajectories and not so smoothly bell-shaped velocity profiles. Therefore, it is important to choose appropriate pulse height value in order to achieve a movement as smooth and straight as possible.

Figure 5 shows that the curvature of movements varies with the direction of reaching. Four movements are simulated at various directions within the working space of the arm. Their movement distances are nearly equal, and the movement time is the same, lasting 0.4 (s). The hand trajectory is straighter in the frontal and the left to right directions than in other directions. Their velocities display similar bell-shaped profiles, indicating an invariant kinematic behavior. The pulse height values for these movements are all in the neighborhood of 0.3 for the shoulder muscles, 0.2 for the biarticular muscles and 0.1 for the elbow muscles. This indicates that control of movement direction is independent of pulse heights.

5.3 Adaptation to changes in moment of inertia

The ability of the motor program to adapt to changes in limb dynamics is evaluated with variations in the moment of inertia of the arm. The motor program may cope with these changes in two ways. The first is to alter descending commands by the motor program itself without invoking the interference of higher centers; and the

A. Hand Movement in Cartesian Space

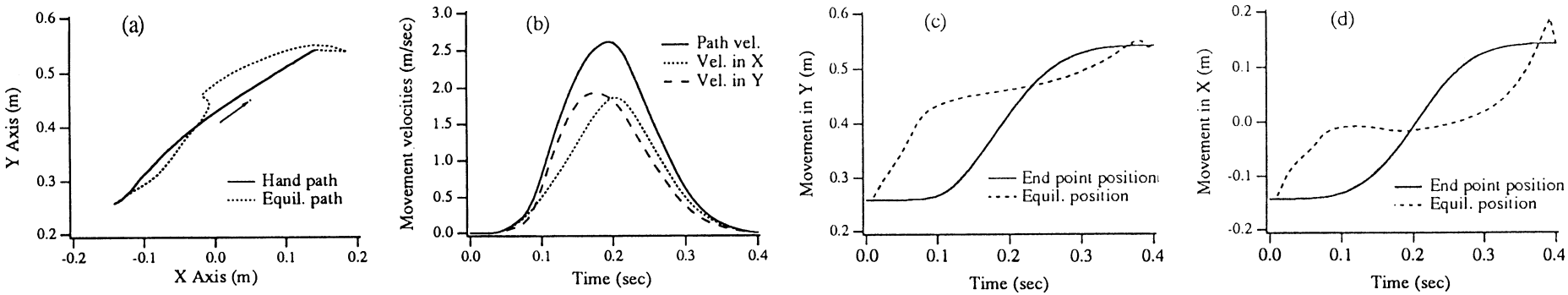

B. Joint Movements

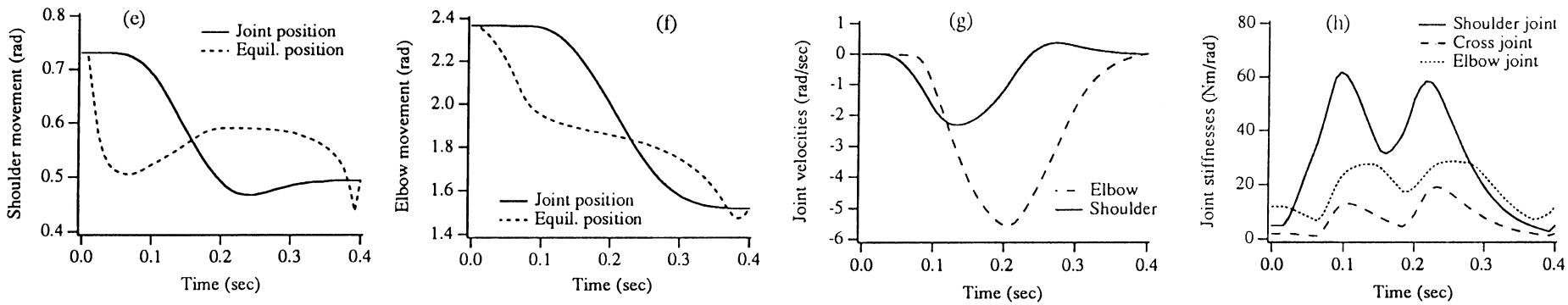

C. Muscle Activations

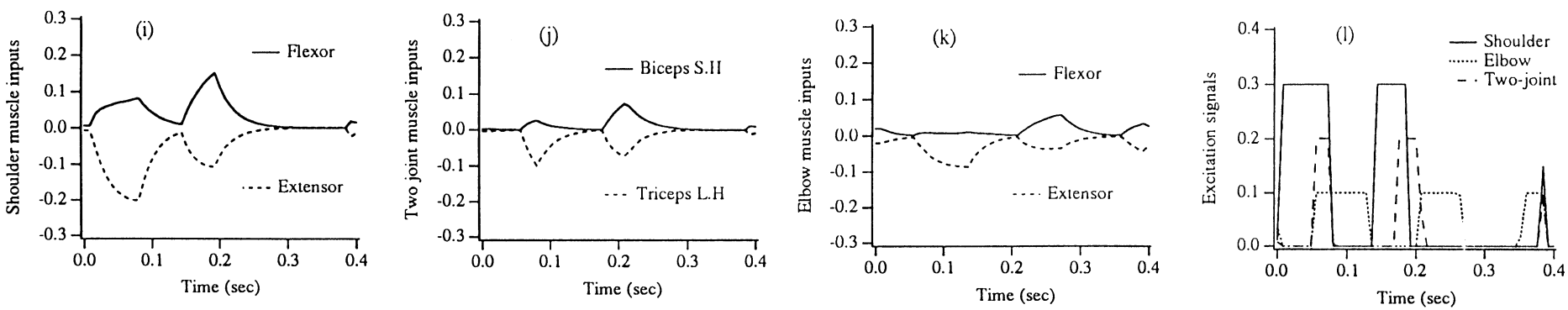

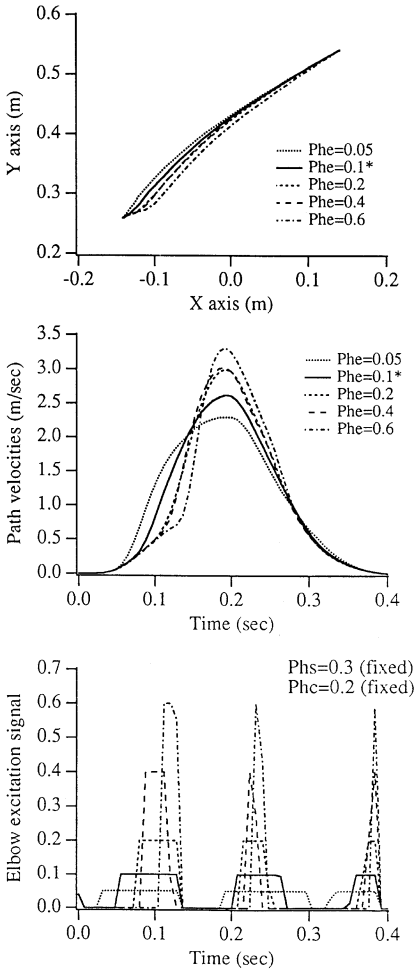

Fig. 4. The effects of elbow pulse height on movement kinematics. The pulse height values for the shoulder and biarticular muscles (*Phs*, *Phc*) are fixed at 0.3 and 0.2, while the elbow pulse height value (*Phe*) varies from 0.05 to 0.6. A value of 0.1 gives the straightest hand path and the smoothest path velocity

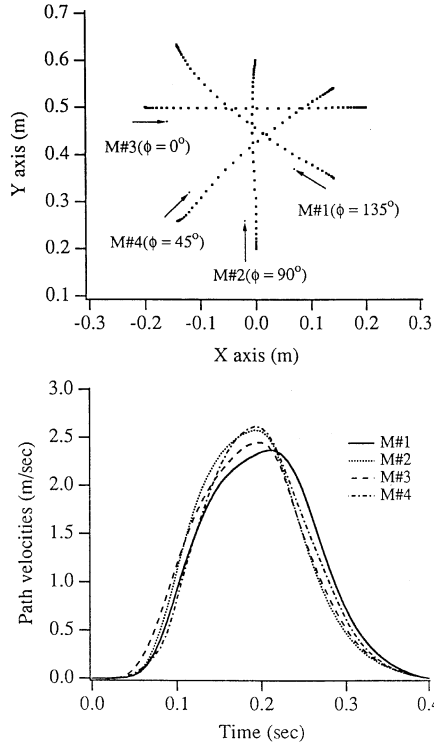

Fig. 5. The movements ($M\#1$, $M\#2$, $M\#3$, $M\#4$) performed in different directions. The durations and distances of these movements are nearly the same. For each movement, tuning is individually performed by varying pulse height values. The smoothest one is chosen to be plotted in the figure. The corresponding pulse height values for the four movements turn out to be similar

second is to do so under the influence of higher centers. Two sets of simulation are performed with (a) fixed pulse heights and (b) varying pulse heights.

Figure 6 shows the results of adaption with and without changes in the pulse heights. The limb inertias of the two segments are changed from the nominal value by -50% to 200%. In Fig. 6A, the values of pulse heights are fixed. It is shown that the perturbed hand movements are close to the nominal one. But their velocity profiles deviate markedly from the nominal velocity. However, deviation in the velocity profile is minimized by adjusting the pulse heights with the changes in limb inertia proportionally, as is clearly illustrated in Fig. 6B. This suggests that the motor program can adapt more effectively to changes in limb dynamics under the influence of the control of higher centers.

5.4 Control of a class of movements

Generation of a class of movements with invariant velocity characteristics is reproduced by model simulation. A class of model-generated movements are shown in Fig. 7. The duration of movements ranges from 0.3 (s) to 1.5 (s). Similarity of movements is evaluated by the normalized hand (end-point) velocity profiles. For each movement, the pulse height values are adjusted so that a similar velocity profile is achieved. In simulation, it is found that for slow movements below 0.6 s of duration a triphasic (or biphasic) burst pattern of excitation will lead to a velocity profile with double peaks. When a constant excitation signal is used, a nicely bell-shaped velocity is obtained. Therefore, for movements below 0.6 s duration a constant excitation signal is employed. In these cases the joint stiffness is fixed; only the equilibrium position is the control variable. Thus, two different strategies are employed for controlling fast and slow movements. A pulsed excitation signal leads to a triphasic activation pattern for fast movements, but a constant excitation signal is required for control of slow movements.

Fig. 3A–C. An optimal movement of 0.4 (ms) duration at a direction of about 45°. **A** The hand movement in Cartesian space is described in (*a*) to (*d*). **B** Joint movements are illustrated in (*e*) to (*h*). **C** Muscle control inputs and the excitation signals are given in (*i*) to (*l*)

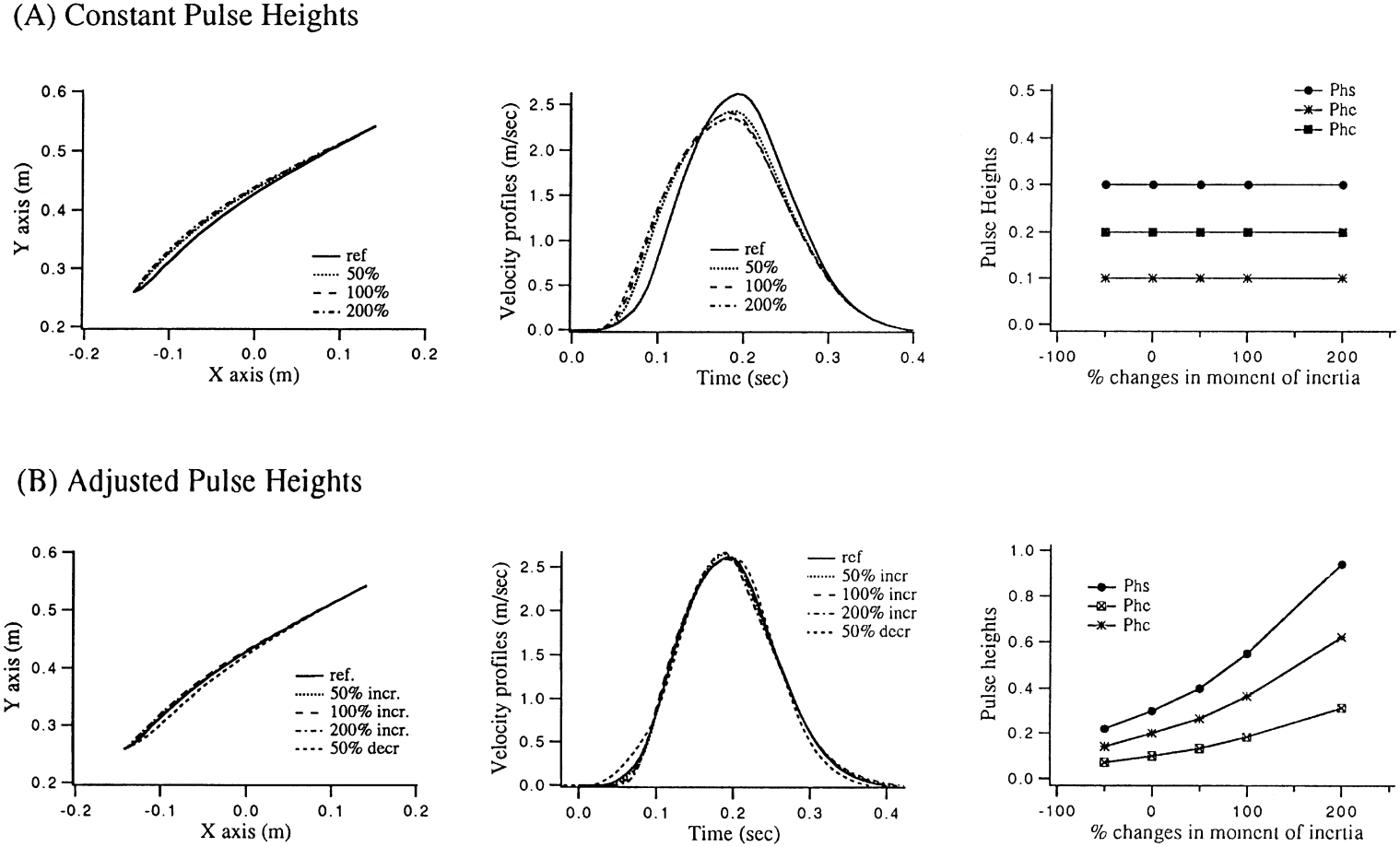

Fig. 6A, B. Adaptation to inertial load changes. The inertia of limb is changed from − 50% to 200% of its nominal values. A − 50% change indicates a decrease from its nominal value by 50%. **A** The pulse height values are fixed a constant levels. **B** The pulse height values are adjusted according to the change in inertia

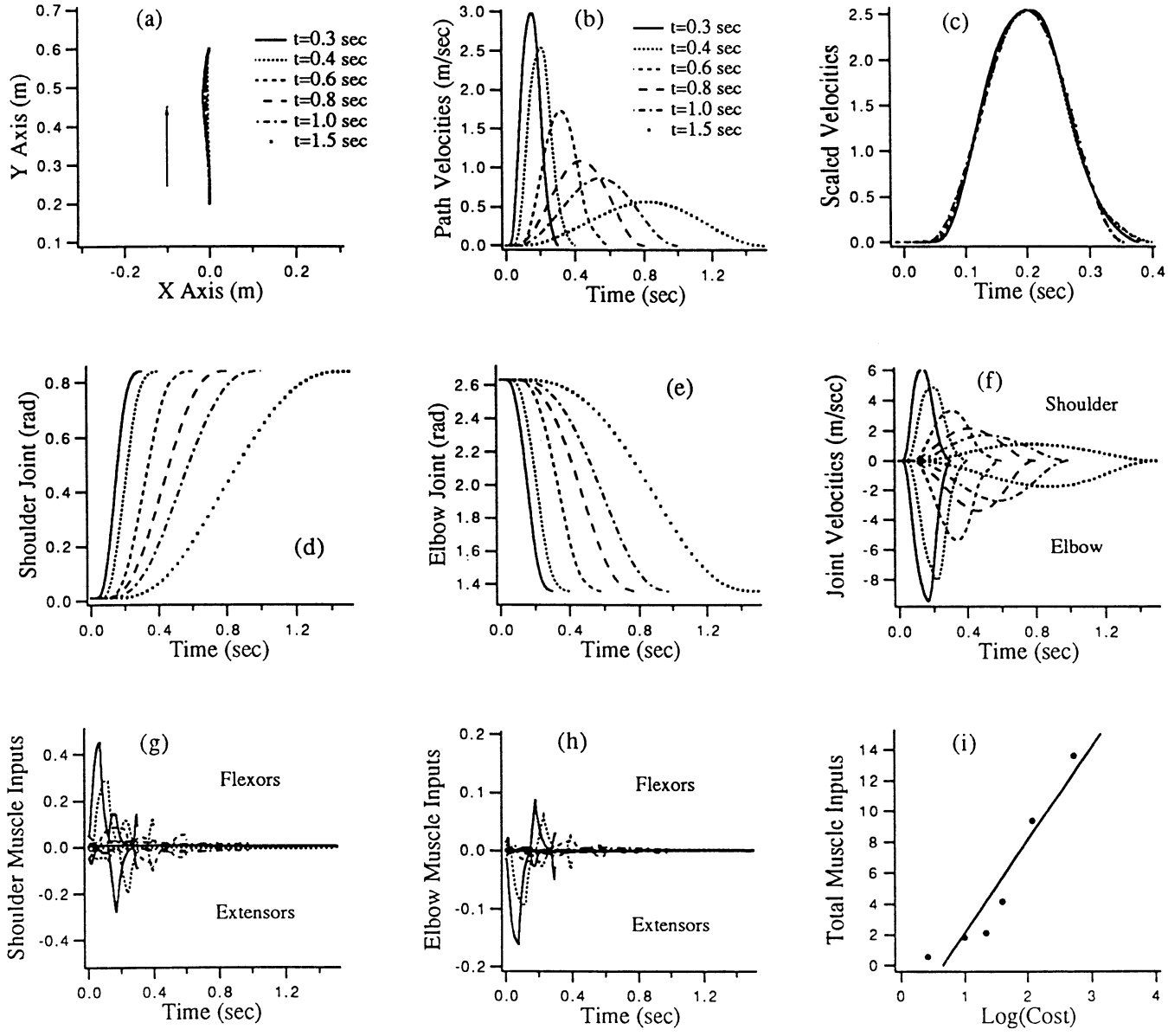

Fig. 7. A family of reaching movements (**a–i**) with varying speeds. Their movement duration (t) ranges from 0.3 s to 1.5 s, i.e. from fast movement to very slow movement. In this direction, the biarticular muscles are not activated for performing movements. Thus, the inputs for biarticular muscles are not plotted

6 Discussions

The complexity associated with control of multi-joint movements arises from the highly redundant and nonlinear dynamics. In neurophysiology, how the brain solves this complex control problem remains a mystery. Due to the similarity in the control problem, revealing the neural control mechanism will have a profound impact on the fields of human rehabilitation and robotics. The conventional notion concerning neural control of movements follows a sequence of inverse computation from movement trajectory to joint torque and to muscle commands. A fatal limitation of this theory is that the inputs to a set of redundant muscle actuators cannot be uniquely determined given a movement trajectory. Thus, inverse computation is not likely for biological movement control. The equilibrium point (EP) model based on the spring- like property of muscle (Houk and Rymer 1981; Hogan, 1985) is gaining wide acceptance as a framework for movement control, because EP control not only alleviates the difficulty of inverse computation but also simplifies the process of computing motor commands. However, the test of the EP hypothesis proves to be a formidable task, due to inaccessibility of central parameters. In many cases, peripheral measurements have to be made to infer central processing of motor commands. In addition, different versions of the EP control model are suggested, which are supported by partial

evidence of the behavior of voluntary arm movements. Therefore, the EP hypothesis remains an attractive theoretical framework and yet receives little support from the large volume of existing experimental data about voluntary arm movements.

The main purpose of this study was to unify the EP theory with experimental data by a new EP control model. A key component of the new model is the inclusion of a spinal network of reciprocal inhibition which links the EP controller to the muscular actuators. In this model, the controller receives instructions from higher centers of the brain, which represent the desired movement in Cartesian space. The objective of the controller is to use as little muscular effort as possible in the execution of a movement, which is evaluated by the cost function of (1). In the spinal cord, the neural network converts descending motor commands into neural inputs to each individual muscle involved in movement production. Reciprocal inhibition has been thought to assist maintenance of joint posture in the face of disturbances. In the new model, however, reciprocal inhibition also plays an important function in the translation of descending commands into muscle inputs. With this relay of motor transformation, the limb will be maintained at a steady posture if a steady equilibrium point is specified, or will be moved from one position to another if a dynamic trajectory of the equilibrium points is computed by the optimal controller. In such a formulation, calculation of muscle inputs requires no inverse computation. Overall, the model describes the complete process of transformation of a motor goal into muscle control inputs that can realize the intended movement.

Numerical results show that the model is capable of reproducing the major characteristics of muscle control and movement kinematics. The model is able to reveal two important aspects of movement control. The first of these is the generation of muscle control signals. A triphasic burst pattern of agonist and antagonist muscle activation is obtained as a result of the minimal effort control strategy (Fig. 3 and others). This stereotyped pattern remains unchanged for movements in different directions and fast movements. It is also shown that this pattern is in keeping with the rhythm of pulsation of the excitation signals, which typically have three pulses. In human arm movements the triphasic muscle activation pattern was observed. Karst and Hasan (1991b) reported triphasic burst electromyographic activities in antagonist muscles during planar two-joint arm movements. It was observed that the amplitude of burst was modulated by the spatial directions of the target position. The agreement with experimental data implies that the minimal effort criterion characterizes the inherent nature of human motor control. For slow movements, the model suggests that it is necessary to use constant excitation signals, rather than the triphasic burst signals, in order to produce a bell- shaped velocity profile. Otherwise, a double-peaked velocity profile appears. Thus, for slow movements, joint stiffness must be kept at a constant level. This fact is also consistent with experimental results. It was found that the variation in joint stiffness during slow movement was much less than that for fast movements (Latash and Gottlieb 1991). Thus it appears that different strategies are necessary for controlling fast and slow movements.

The second important aspect of movement control is the regulation of kinematics. The analysis of results indicates that although the gross features of a movement are prescribed by the optimal controller, the details of velocity profiles can be fine-tuned by varying the maximal levels of excitation signals, or the pulse heights, which are direct inputs to the optimal controller from higher centers of the brain. These inputs provide an independent channel for the brain to adjust movement kinematics separately. By this means, a preference for a particular kinematic behavior can be achieved, and an invariant velocity profile can be preserved by selecting appropriate pulse height values. Such an ability allows adaptation to different movement speeds and different loading conditions, so that a unified kinematic feature for all movements is possible. Adaptation to inertial load changes and the scaling property of voluntary arm movements are clearly reproduced by using pulse height modulation, as shown in Figs. 6 and 7. The gross features of hand movement are similar to those described by measurement of human trajectories. The hand movement follows a near-straight (but not perfectly straight) path in Cartesian space with a bell-shaped velocity (Fig. 3). It is also shown that the optimal hand paths are not so sensitive to changes in muscle activation patterns as is depicted in Fig. 4. Thus, only fine-tuning is necessary in order to obtain a similar velocity profile for a class of movements. The analysis indicates that to achieve an invariant velocity profile, only a global tuning variable needs to be adjusted. No explicit formulation of movement trajectory is required.

Another interesting result from the model is that there is a fixed sequence of activation from proximal to distal muscles in the arm. In the initiation of movement, the shoulder agonist muscle is always activated earlier than the elbow agonist. In Fig. 3 there is a 40 (ms) delay between the activation of the shoulder muscle and the elbow muscle. This delay varies with the direction and speed of movements. This delay is reported in experimental observations made by Karst and Hasan (1991a,b), who studied arm movement initiation in different directions, and found that for most target directions initial electromyographic activity at the shoulder preceded that at the elbow by 5–40 (ms). It was concluded that this delay could not be due to nerve conduction, but must be the result of the control strategy of the brain.

Appendix. Model parameters

Model parameters used in the simulation are summarized here.

Limb parameters
Limb segment masses:

$$m_1 = 1.97 \text{ (kg)} \quad m_2 = 1.64 \text{ (kg)}$$

Limb segment inertias:

$$I_1 = 0.0130\ (\mathrm{kg\,m^2}) \quad I_2 = 0.0250\ (\mathrm{kg\,m^2})$$

Limb segment lengths:

$$L_1 = 0.36\ (\mathrm{m}) \quad L_2 = 0.41\ (\mathrm{m})$$

Muscle parameters
Muscle stiffness torque ratio and passive torques:

$$m_{ij} = 0.5\ (\mathrm{rad}), \quad b_{ij} = 1.0\ (\mathrm{N\,m})$$

(for $i = 1, 2, 3$ and $j = \mathrm{f}, \mathrm{e}$)

Muscle maximum stiffnesses and activation time constants:

$$n_{ij} = 250\ (\mathrm{N\,m/rad}), \quad \tau_{ij} = 0.05\ (\mathrm{s})$$

(for $i = 1, 2, 3$ and $j = \mathrm{f}, \mathrm{e}$)

Spinal process parameters
Reciprocal inhibition gains:

Single-joint muscles:

$$r_{ij} = 1.0\ (\mathrm{rad}^{-1}) \quad (\text{for } i = 1, 2 \text{ and } j = \mathrm{f}, \mathrm{e})$$

Biarticular muscles:

$$r_{3j} = 0.5\ (\mathrm{rad}^{-1}) \quad (\text{for } j = \mathrm{f}, \mathrm{e})$$

Excitation time constants:

$$\tau_{N_i} = 0.029\ (\mathrm{s}) \quad (\text{for } i = 1, 2, 3)$$

Acknowledgements. This work was supported by grants from the Li Foundation, San Francisco, USA, the Chinese Natural Science Foundation (No. 39500038), from the Whitaker Foundation and the Pittsburgh Supercomputing Center of USA.

References

Abend W, Bizzi E, Morasso P (1982) Human arm trajectory formation. Brain 105:331–348

Atkeson CG, Hollerbach JM (1985) Kinematic features of unrestrained vertical arm movements. J Neurosci 5:2318–2330

Bernstein N (1967) The coordination and regulation of movements. Pergamon Press, Oxford

Bizzi E, Hogan N, Mussa-Ivaldi FA, Giszter S (1992) Does the nervous system use equilibrium-point control to guide single and multiple joint movements? Behav Brain Sci 15:603–613

Cannon SC, Zahalak GI (1982) The mechanical behavior of active human skeletal muscle in small oscillations. J Biomech 15:111–121

Carter RR, Crago PE, Keith MW (1993) Stiffness regulation by reflex action in the normal human hand. J Neurophysiol 64: 105–118

Corcos DM, Gottlieb GL, Agarwal GC (1989) Organizing principles for single joint movements. II. A speed-sensitive strategy. J Neurophysiol 62:358–368

Feldman AG (1986) Once more on the equilibrium-point hypothesis (λ-model) for motor control. J Motor Behav 18:17–54

Feldman AG, Orlovsky SV (1972) The influence of different descending systems on the tonic stretch reflex in the cat. Exp Neurol 37:481–494

Flanders M, Pellegrini JJ, Soechting JF (1994) Spatial/temporal characteristics of a motor pattern for reaching. J Neurophysiol, 71:811–813

Flash T (1987) The control of hand equilibrium trajectories in multi-joint arm movements. Biol Cybern 57:257–274

Flash T, Hogan N (1985) The coordination of arm movements: an experimentally confirmed mathematical model. J Neurosci 5: 1688–1703

Ghez C, Martin JH (1982) The control of rapid limb movement in the cat, III. agonist-antagonist coupling. Exp Brain Res 45:115–125

Gottlieb GL, Corcos DM, Agarwal GC (1989) Organizing principles for single joint movements. I. A speed-insensitive strategy. J Neurophysiol 62:342–357

Hannaford B, Stark L (1985) Roles of the elements of the tri-phasic control signal. Exp Neurol 90:619–634

Hannaford B, Stark L (1987) Late agonist activation burst (PC) required for optimal head movement: a simulation study. Biol Cybern 57:321–330

Hasan Z (1986) Optimized movement trajectories and joint stiffness in unperturbed, inertially loaded movements. Biol Cybern 53: 373–382

Hasan Z (1991) Biomechanics and the study of multijoint movements. In: Humphrey DR, Freund H-J (eds) Motor control: concepts and issues. Wiley, New York

Hildreth EC, Hollerbach JM (1987) Artificial intelligence: computational approach to vision and motor control. In Mountcastle VB, Plum F, Geiger SR (eds) Handbook of physiology, Sect 1, The nervous system. High functions of the brain, vol. 5. American Physiological Society, Bethesda, Md

Hogan N (1985) The mechanics of multi-joint posture and movement. Biol Cybern 52:315–331

Hogan N (1988) Planning and execution of multijoint movements. Can J Physiol Pharmacol 66:508–517

Houk JC, Rymer WZ (1981) Neural control of muscle length and tension. In: Brooks VB (ed) Handbook of physiology, sect. 1, The nervous system, vol II, part 1. American Physiological Society, Bethesda, MD, pp 257–324

Karst GM, Hasan Z (1991a) Initiation rules for planar, two-joint arm movements: agonist selection for movements throughout the work space. J Neurophysiol 66:1579–1593

Karst GM, Hasan Z (1991b) Timing and magnitude of electromyographic activity for two joint arm movements in different directions. J Neurophysiol 66:1594–1604

Katayama M, Kawato M (1993) Virtual trajectory and stiffness ellipse during multijoint arm movement predicted by neural network models. Biol Cybern 69:353-362

Kawato M, Maeda Y, Uno Y, Suzuki R (1990) Trajectory formation of arm movement by cascade neural network model based on minimum torque-change criterion. Biol Cybern 62:275–288

Kearney RE, Hunter IW (1990) System identification of human joint dynamics. CRC Crit Rev Biomed Eng 18:55–87

Lan N, Crago PE, (1994) Optimal control of antagonistic muscle stiffness during voluntary movements. Biol Cybern 70:397–405

Latash ML, Gottlieb GL (1991) Reconstruction of shifting elbow joint compliant characteristics during fast and slow movements. Neuroscience 43:697–712

Lestienne F (1979) Effects of inertial load and velocity on the braking process of voluntary limb movements. Exp Brain Res 35:407–418

Marsden CD, Obeso JA, Rothwell JC (1983) The function of the antagonistic muscle during fast limb movements in man. J Physiol (Lond) 335:1–13

Morasso P (1981) Spatial control of arm movements, Exp Brain Res 42:223–227

Paul RP (1981) Robot manipulators: mathematics, programming and control. MIT Press, Cambridge, Mass

Seif-Naraghi AH, Winters JM (1990) Optimized strategies for scaling goal-directed dynamic limb movements. In: Winters JM, Woo S (eds) Multiple muscle systems, biomechanics and movement organization. Springer, Berlin Heidelberg New York

Shadmehr R, Mussa-Ivaldi FA (1994) Adaptive representation of dynamics during learning of a motor task. J Neurosci 14:3208–3224

Uno Y, Kawato M, Suzuki R (1989) Formation and control of optimal trajectory in human multijoint arm movement: minimum torque-change model. Biol Cybern, 61:89–101

Wallace SA (1981) An impulse-timing theory for reciprocal control of muscular activity in rapid, discrete movements. J Mot Behav, 13:144–160